Identification of dynamic properties of a turboset rotor from its rundown

Balda M.

Institute of Thermomechanics, Academy of Sciences, Veleslavínova 11, 301 14 Plzeň, Czech Republic

This contribution deals with a problem of an identification of natural frequencies and modes of vibrations by processing run-down data measured at many points of the turboset. A data matrix is assembled out of a vector of speeds, and vectors of corresponding amplitudes and phases of vibrations measured at every measuring point. A physical distribution of unbalances along the rotor is unknown, however, it is assumed to be constant during the run-down of the machine. This assumption allows considering the turboset under observation as a Single-Input-Multiple-Output (SIMO) system. The processing of data may proceed in two stages. The first stage performed in the frequency domain includes processing of data from single points of measurement as Single-Input-Single-Output (SISO) systems using rough initial estimates of natural frequencies calculated from global information on resonance peaks. This step of processing may serve as a modal filter of noisy data. The other step processes rough or filtered data by a global time domain procedure. The results are natural frequencies with corresponding damping and modes of vibrations. The results serve both for the operation of the machine, and comparing the fit of the mathematical model.

1. Introduction

A reliability of any technical system becomes a necessity owing to the hard competition on the market. If the system is a nuclear power plant, a requirement of the total reliability must be fulfilled without any exception. This is the reason why high attention is paid to measurements of dynamic properties of all important parts of the plant. Moreover, the measurements could serve as a reference for the future operational diagnostics.

A rotor of a turboset is a typical mechanical system that is excited by centrifugal forces. They are generated by rotating unbalance masses distributed at random along the rotor length due to residual excentricity of centers of gravity according to its rotational axis. The dynamic forces are deflecting the rotor, which starts to vibrate. Levels of acceptable vibrations are limited by international standards, since they may have a damaging effect on the rotor and its environment. The influence of dynamic forces is amplified if the rotor runs near to its natural frequencies. Those bands of excessive vibrations are known as critical speeds. This is the reason why natural frequencies and corresponding modes of vibrations belong to the most important dynamic properties of the rotor.

2. Frequency response of a discrete system

Let us assume the rotor being a linear system with multiple inputs and multiple outputs (MIMO). Should the rotor be discretized, its behavior is described by the well known ordinary linear differential equation

$$\boldsymbol{M}\,\ddot{\boldsymbol{q}}(t) + \boldsymbol{B}\,\dot{\boldsymbol{q}}(t) + \boldsymbol{K}\,\boldsymbol{q}(t) = \boldsymbol{f}(t). \tag{1}$$

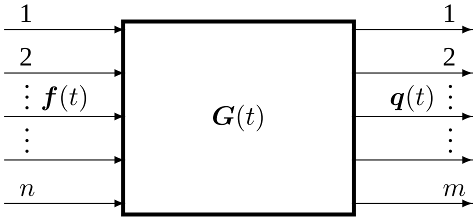

Figure 1: MIMO system

The Fourier transform of the Equation (1) with trivial initial conditions yields

$$\boldsymbol{q}(p) = \boldsymbol{G}(p)\,\boldsymbol{f}(p)\,, \tag{2}$$

where $p = i\omega = i2\pi f$ is a scaled frequency parameter. For the sake of simplicity, the symbols $\boldsymbol{f}$ and $\boldsymbol{q}$ were used both for vectors of time functions and their Fourier transforms. The properties of the functions are than strictly joined with their arguments. The matrix $\boldsymbol{G}(p)$ is a *frequency response matrix* of the system corresponding the Equation (1), and has the form

$$\boldsymbol{G}(p) = [\,p^2\,\boldsymbol{M} + p\,\boldsymbol{B} + \boldsymbol{K}\,]^{-1} = \mathcal{F}\{\boldsymbol{G}(t)\}, \tag{3}$$

An original to the matrix $\boldsymbol{G}(p)$, an inverse Fourier transform of the matrix $\boldsymbol{G}(p)$, is the matrix $\boldsymbol{G}(t) = \mathcal{F}^{-1}\{\boldsymbol{G}(p)\}$. It is a matrix of the rotor responses to Dirac impulses, the *impulse response matrix*. The original to the Equation (2) is

$$\boldsymbol{q}(t) = \int_{-\infty}^{\infty} \boldsymbol{G}(\tau)\,\boldsymbol{f}(t-\tau)\,d\tau \;=\; \boldsymbol{G}(t) * \boldsymbol{f}(t) \tag{4}$$

known as a *convolution* of the impulse response matrix with a vector of excitations. It can be proved that the matrix $\boldsymbol{G}(p)$ may be expressed also in in terms of modal matrices $\boldsymbol{V}$ and $\boldsymbol{W}$ and a spectral matrix the form (see Appendix A)

$$\boldsymbol{G}(p) = \boldsymbol{V}_q\,[\,p\,\boldsymbol{I}_{2n} - \boldsymbol{S}\,]^{-1}\,\boldsymbol{W}_q^H \tag{5}$$

Centrifugal forces acting on the rotor do not possess a general character. They depend on an unbalance $\boldsymbol{u}$ linearly, and on speed quadratically. A constant *unknown* unbalance $\boldsymbol{u}$ rotating at a speed corresponding the frequency parameter p_k generates steady harmonic excitation $\boldsymbol{f}(p_k)$ that causes a steady harmonic response $\boldsymbol{q}(p_k)$ described by the formulae

$$\boldsymbol{f}(p_k) = -p_k^2\,\delta(p-p_k)\,\boldsymbol{u} \qquad and \qquad \boldsymbol{q}(p_k) = \boldsymbol{q}(p)\,\delta(p-p_k)\,, \tag{6}$$

respectively. Both functions contain the Dirac impulse $\delta(p{-}p_k)$ on the imaginary frequency p_k. It may be removed from both sides of the Equation (25) giving thus

$$\boldsymbol{q}(p_k) = -\boldsymbol{V}_q\,\left[\,p_k^2\,(p_k\boldsymbol{I} - \boldsymbol{S})^{-1}\right]\,\boldsymbol{W}_q^H\,\boldsymbol{u} \tag{7}$$

3. Local identification of critical speeds

A method for the identification of SISO systems from the frequency response function was developed by Kozánek many years ago (see [1]). We have adapted the method for the excitation by an unbalance.

The most simple measurement of rotor vibrations is taken in one (i-th) measuring point during very slowly changing speed of rotation. The measured data should be built out of triples of values, which are speed and a pair of vibration parameters. Those may be either amplitude and phase, or real and imaginary parts of vibrations. In both cases they determine a complex value $q_i(p_k)$ of vibration under the measured speed corresponding p_k, which may be obtained from the Equation (7):

$$q_i(p_k) = -\sum_\nu \frac{p_k^2}{p_k - s_\nu}\,\underbrace{\{\,\boldsymbol{v}_i^H\}_\nu\{\boldsymbol{W}_q^H\boldsymbol{u}\}_\nu}_{-a_{i\nu}} \;=\; \sum_\nu \frac{p_k^2}{p_k - s_\nu}\,a_{i\nu} \tag{8}$$

The factors $a_{i\nu}$ as coefficients of the linear combination of “resonant terms” determine a degree of modal affinity of the unknown unbalance $\boldsymbol{u}$. The harmonic response $q_i(p_k)$ is thus a linear combination of modal contributions of the unbalance. Hence, responses of the rotor in the measuring point depend on $2n$ unknowns, s_ν and $a_{i\nu}$, while p_k is the independent variable, speed. In such a way, the unknown unbalance $\boldsymbol{u}$ entered another vector of unknown sensitivities $\boldsymbol{a}_\nu$ of the rotor in the measuring point to be identified simultaneously with eigenvalues s_ν.

In order to diminish the influence of modes not involved into the identification, the expression for the measured response $\hat{q}_i(p_k)$ has been appended by a correction term, giving thus

$$\hat{q}_i(p_k) \approx \sum_\nu \frac{p_k^2}{p_k - s_\nu}\,a_{i\nu} + \frac{h}{p_k} \tag{9}$$

The main purpose of the correction term is to compensate a position of the origin with respect to the lowest frequencies. Its influence declines with raising frequency. The quantity h is a new unknown to be identified as well. The identification is based on the least-squares method using Newton-Raphson algorithm for minimization of the scalar function $S = \boldsymbol{r}^H\boldsymbol{r}$, sum of squares of residual modules as differences between identified function values and measured $\hat{q}_i(p_k)$:

$$r_{ki} = \sum_\nu \frac{p_k^2}{p_k - s_\nu}\,a_{i\nu} + \frac{h}{p_k} - \hat{q}_i(p_k) \tag{10}$$

A vector of unknown parameters $\boldsymbol{c} = [\,\boldsymbol{s}^T,\,\boldsymbol{a}_i^T,\,h\,]^T$ is found by iterations (ℓ) as

$$\boldsymbol{c}_i^{(\ell+1)} = \boldsymbol{c}_i^{(\ell)} - \left[\boldsymbol{J}^{(\ell)}\right]^+\boldsymbol{r}^{(\ell)}\,, \tag{11}$$

with the Jacobian matrix

$$\boldsymbol{J} = \left[\frac{\partial \boldsymbol{r}}{\partial \boldsymbol{s}}, \frac{\partial \boldsymbol{r}}{\partial \boldsymbol{a}}, \frac{\partial \boldsymbol{r}}{\partial h} \right] = [\, \boldsymbol{J}_s, \, \boldsymbol{J}_a, \, \boldsymbol{J}_h \,] = \left[\left[\left[\frac{p_k^2}{(p_k - s_\nu)^2} \, a_\nu \right], \left[\frac{p_k^2}{p_k - s_\nu} \right], \boldsymbol{p}^+ \right] \right. \tag{12}$$

The symbol + in the position of a superscript designates a pseudo-inversion of an object. Both submatrices $\boldsymbol{J}_s$ and $\boldsymbol{J}_a$ have n columns and as many rows as is the number of measuring frequencies

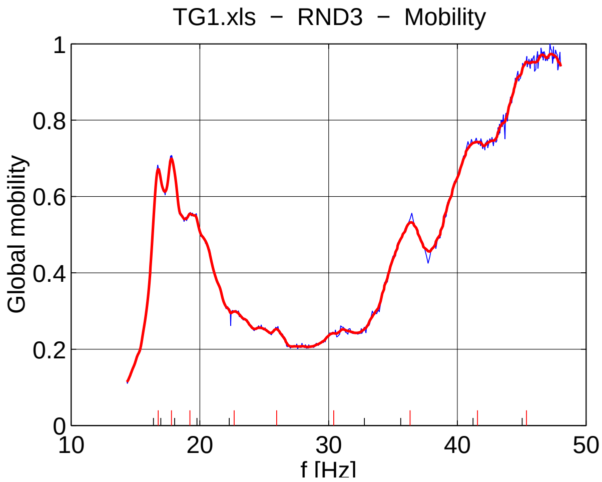

Figure 2: Total relative mobility

Initial estimates of the unknowns are determined automatically before starting the optimization procedure. The eigenvalues s_ν are estimated from the positions of the amplitude peaks of the smoothed mobility which is the function $\sum_i p_k |\, q_i(p_k) \,|$ (see Fig. 2). There are two curves plotted in the figure. The curled line corresponds to the measurement, while the smoothed one served for finding frequencies of peaks.

A better estimate is then found from the approximation of the response (9) by fitting it to five points of measurement gathered round the peak point p_m. It has been derived from the Equation (9) that

$$p_k^2 \, a_{i\nu} + \hat{q}_i(p_k) \, s_\nu + \frac{p_k - s_\nu}{p_k} \, h \approx p_k \, \hat{q}_i(p_k) \tag{13}$$

Hence, the initial estimate $\hat{\boldsymbol{c}}$ of the vector $\boldsymbol{c}$ of unknowns may be found in the form of solution of the system of overdetermined linear algebraic equations composed out of Equation (13) applied for frequencies p_ℓ up to p_h, where p_m is the peak amplitude $|\, q_i(p_m) \,|$ frequency, $\ell = m{-}2$ and $h = m{+}2$:

$$\begin{bmatrix} \hat{s}_\nu \\ \hat{a}_\nu \\ \hat{h} \end{bmatrix} = \begin{bmatrix} 1\,, & \dfrac{p_\ell^2}{q(p_\ell)}\,, & \dfrac{p_\ell - s_\nu}{p_\ell \, q(p_\ell)} \\ \vdots & \vdots & \vdots \\ 1\,, & \dfrac{p_h^2}{q(p_h)}\,, & \dfrac{p_h - s_\nu}{p_h \, q(p_h)} \end{bmatrix}^+ \begin{bmatrix} p_\ell \\ \vdots \\ p_h \end{bmatrix} .$$

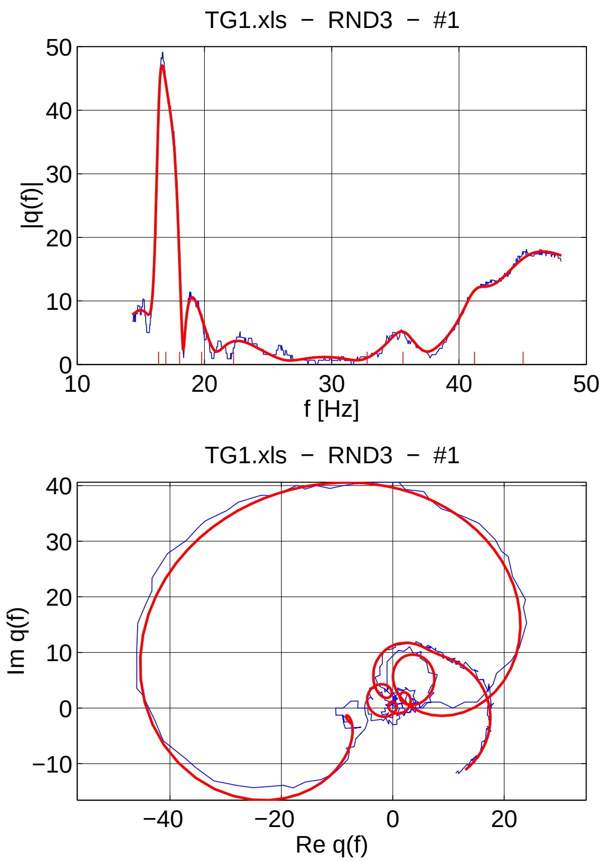

Figure 3: Measured and identified response

The Figure 3 shows results of the identification of critical speeds from data measured on a single bearing housing and collected by a computer controlled data acquisition system.

The upper subfigure displays amplitudes in course of the rotational frequency. The noisy line has been measured, the smoothed one shows the identified response. Short lines above the frequency axis belong to real parts of identified eigenvalues.

A variation of the rotor response to the unknown unbalance is shown in the complex plane in the lower subfigure. It is clear that the identified response fits the measured one quite well.

Further, a part of a protocol on processing is presented which shows that the input data have been stored in the Excel-file TG1.xls and its sheet denoted RND3. The tolerance for the peak recognition has been chosen 12% which means that only the peaks of the smoothed mobility higher by more than 12% compared with their neighborhoods are accepted as the real peaks. Number of equal-weight 3-point smoothing cycles has been chosen equal 10. A speed step for plotting the identified response has been 3 rpm.

4. Global identification of critical speeds and modes

```
==========================================
 Critical speed identification 20/01/2002
==========================================

       file  = TG1.xls =>
       sheet = RND3 =>
       tolpeak % =   12.0000 =>
       delta rpm =    3.0000 =>
       n-smooth  =   10.0000 =>

  Exe time =   59.025 [s]

  n        f(n)             b_r(n)    Q(n)

  1  16.3960  -0.3842*i   0.0234   21.37
  2  16.9683  -2.1123*i   0.1235    4.05
  3  18.0453  -0.4943*i   0.0274   18.25
  4  19.7736  -2.3565*i   0.1183    4.23
  5  22.2887  -4.4024*i   0.1938    2.58
  6  32.7860  -6.4256*i   0.1923    2.60
  7  35.6061  -1.2332*i   0.0346   14.45
  8  41.2155  -1.2275*i   0.0298   16.78
  9  45.0380  -3.8167*i   0.0844    5.92
```

The local identification described in the foregoing section does not guarantee that all critical speeds will be identified, and that they will get the same values from all points of measurements. Mutual differences could be quite large. This is the reason why global methods processing the total measured information were sought. One of them belongs to Heylen et all. Unfortunately, it is difficult to understand the description of the method named LSCE in [2]. Let us derive a similar modified method [3].

The original to the frequency response matrix $\boldsymbol{G}(p)$ given by the equation (27) is an impulse response matrix $\boldsymbol{G}(t)$. It describes dynamic properties of the system under observation as good as the matrix $\boldsymbol{G}(p)$. The inverse Fourier transform of $\boldsymbol{G}(p)$ is (with omitted subscript q with $\boldsymbol{V}$ and $\boldsymbol{W}$)

$$\boldsymbol{G}(t) \;=\; \int_{-\infty}^{\infty} \boldsymbol{G}\,(p)\, e^{+i2\pi f t} df \;=\; \boldsymbol{V} \exp(\boldsymbol{S}t)\, \boldsymbol{W}^H \,, \tag{15}$$

where $\exp(\boldsymbol{S}t)$ is a matrix exponential of the t-multiple of the spectral matrix $\boldsymbol{S}$, $\exp(\boldsymbol{S}t) = \mathrm{diag}\,[\exp(s_\nu t)\,]$. The experimental data are not continuous but sampled functions. Results of the sampling are time- or frequency-series dependent on a sampling period T or a sampling frequency f_s. The general Fourier transforms are then replaced by their discrete variants (DFT, IDFT). Hence, the last equation takes the form of a matrix time series:

$$\boldsymbol{G}(kT) \;=\; \boldsymbol{V} \exp(k\boldsymbol{S}T)\, \boldsymbol{W}^H, \qquad k \;= 0, \ldots, N-1\,. \tag{16}$$

The variable N is the number of samples in every elementary time series. While the continuous response of a causal linear system to the general excitation has the form

$$\boldsymbol{q}(t) \;=\; \boldsymbol{G}(t) * \boldsymbol{f}(t) \;=\; \int_0^t \boldsymbol{G}(\tau)\, \boldsymbol{f}(t-\tau)\, d\tau \;=\; \int_0^t \boldsymbol{G}(t-\tau)\, \boldsymbol{f}(\tau)\, d\tau \,, \tag{17}$$

the sampled variant of it is

$$\boldsymbol{q}(kT) \;=\; T \sum_{\kappa=0}^{k} \boldsymbol{G}((k-\kappa)T)\, \boldsymbol{f}(\kappa T) \;=\; T\boldsymbol{V} \sum_{\kappa=0}^{k} \exp((k-\kappa)\boldsymbol{S}T)\, \boldsymbol{W}^H\, \boldsymbol{f}(\kappa T). \tag{18}$$

This formula will be used extensively for a derivation of the global identification method which yields the matrices $\boldsymbol{S}$, $\boldsymbol{V}$ and $\boldsymbol{W}$ (see Appendix B). Critical speeds are the imaginary parts of the eigenvalues s_ν while modal dampings are $b_\nu = -Re\; s_\nu / |\, s_\nu\,|$. Natural modes of the rotor vibration are columns of the modal matrix $\boldsymbol{V}$.

Several remarks

A. The general description of the identification method has been based on the assumption that the matrix frequency series $\boldsymbol{G}(p)$ is known and that the transfer of the excitation $\boldsymbol{f}(p)$ to the response is described by the Equation (25). Unfortunately, we measure only responses caused by an unknown unbalance $\boldsymbol{u}$, that is

$$\boldsymbol{q}(p) = \boldsymbol{G}(p)\, \boldsymbol{f}(p) \;=\; -p^2\, \boldsymbol{G}(p)\, \boldsymbol{u} \tag{19}$$

If we accept the current unbalance as a unit in the measured run, the frequency response matrix becomes $\boldsymbol{G}(p) = \boldsymbol{q}(p)/p^2$. It is a column vector of dimension N in case of discrete systems. Consequently, all matrices $\boldsymbol{F}$ and the modal matrix $\boldsymbol{W}$ are of the order one in this case.

B. The measured data are sometimes injured by measuring noise. The direct processing of the whole collection of data might be uncertain. In this case, it is possible to filter out the noise via step by step identification of all single points as SISO systems. Afterwards, we use the reconstructed filtered data as an input for the global procedure.

C. A protocol made during the data processing of a measurement taken in twelve places simultaneously is presented below. The program is interactive. It allows the user to input his values of variables behind the sign =>. If no new value has been input, the default value is accepted. The second possibility of the program control lies in the variable JOB, which may be set by the user to several three-character strings that are recognized by a program switch as commands.

```
============================================================
   Critical speed identification     22-Jan-2002
============================================================

          file   = TG1.xls =>
          sheet = RND3 =>
          tolpeak % =    12.0000 =>
          delta rpm =     3.0000 =>
          n-smooth  =    10.0000 =>
          ini peak #=     2.0000 =>

 Frequencies found in Sum(|q(f)|*f)/max(|q(f)|*f)

          f( 1) = 16.767 [Hz]
          f( 2) = 17.800 [Hz]
          f( 3) = 19.233 [Hz]
          f( 4) = 22.667 [Hz]
          f( 5) = 25.967 [Hz]
          f( 6) = 30.400 [Hz]
          f( 7) = 36.333 [Hz]
          f( 8) = 41.567 [Hz]
          f( 9) = 45.367 [Hz]

          JOB   = glo =>

          JOB   = ide =>
          nf    =   11 => 10
          p     =   20 =>

   Identified values:

  k          f(k)                   n(k)          b_p(k)      Q
            [Hz]                   [rpm]

  1  15.7129  -0.6294*i     942.78  -37.76*i   0.0400   12.49
  2  16.9152  -0.5089*i    1014.91  -30.53*i   0.0301   16.63
  3  18.7301  -1.0926*i    1123.80  -65.56*i   0.0582    8.59
  4  20.3696  -1.4223*i    1222.17  -85.34*i   0.0697    7.18
  5  26.0886  -1.6570*i    1565.31  -99.42*i   0.0634    7.89
  6  30.9713  -2.8076*i    1858.28 -168.46*i   0.0903    5.54
  7  35.2757  -1.2567*i    2116.54  -75.40*i   0.0356   14.04
  8  40.4713  -1.6340*i    2428.28  -98.04*i   0.0403   12.39
  9  48.0000  -1.3580*i    2880.00  -81.48*i   0.0283   17.68
```

D. There are differences between the identification results gained from the local and global approaches. They can easily occur as seen from Fig. 5 which shows modules of all measured responses at once. The local approach may give different eigenvalues at different points of measurement.

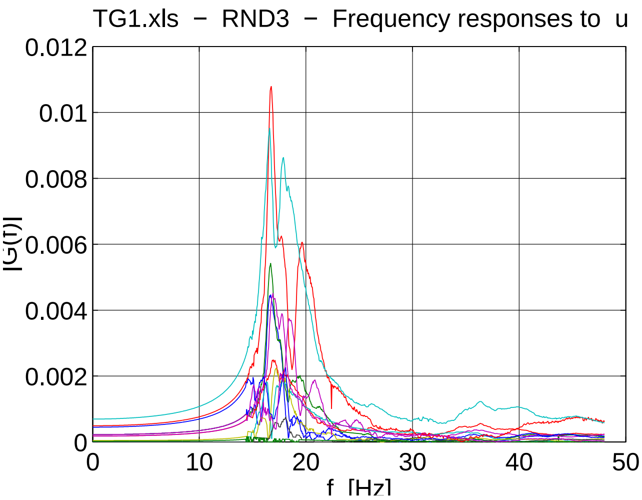

Figure 4: Measured responses in individual points

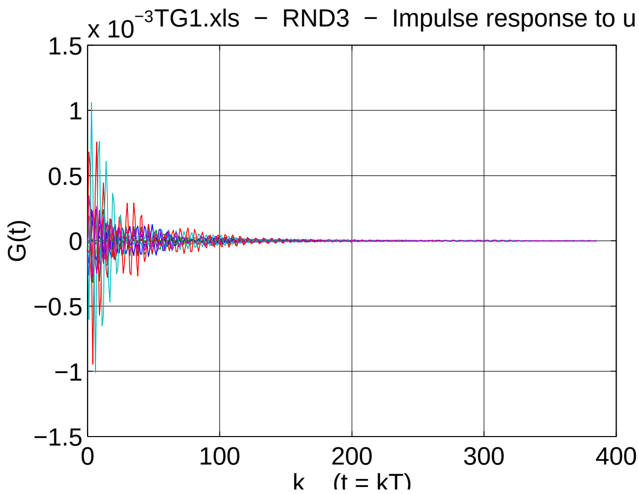

Figure 5: Impulse responses in individual points

E. The Figure 5 shows the impulse responses $\boldsymbol{G}(kT)$ to the unknown unbalance. They have been obtained via FFT from $\boldsymbol{G}(f_s n/N)$. The Fourier transform needs to have the data of $\boldsymbol{G}(f_s n/N)$ distributed regularly with constant frequency step over the whole frequency interval, zero frequency included. However, the measurement started at a higher frequency, about 600 rpm in our case. Hence, it was necessary to reconstruct data at the beginning of the frequency interval. Since the influence of damping may be omitted far from the critical speeds, the non-measured responses have been calculated using the formulae

$$\boldsymbol{g}(0) = (1 - p_x/p_m)^2\, \boldsymbol{g}(p_m) \qquad \text{and} \qquad \boldsymbol{g}(p_k) = \frac{\boldsymbol{g}(0)}{1-(p_k/p_m)^2} \qquad \text{for} \qquad 0 <= k < m, \tag{20}$$

where p_x is the frequency of the first resonance peak and p_m the lowest frequency of the measurements.

G. One of twelve natural modes is plotted in the Fig. 6. The best insight into the modes may be obtained by animation of modes after the global identification.

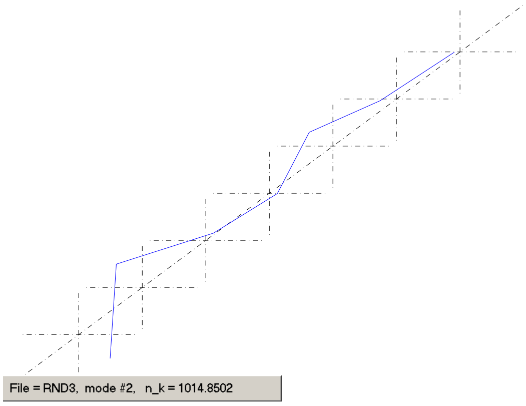

Figure 6: 2nd natural mode of the rotor

5. Conclusions

This paper deals with three approaches to the problem of an identification of dynamic properties of rotors based on run-down vibration data. Non of them requires any knowledge of the unbalance that generated measured vibrations.

The first method is based on the local identification of critical speeds. It yields eigenfrequencies observable at the measured point. They are natural frequencies and corresponding damping. The second method gives a global estimation of eigenvalues and modes by processing matrix time series of impulse responses. The third method is a combination of both methods. The local identification serves as a modal filter for input data, and the global method returns the final identified frequencies, dampings and modes.

The described procedure can serve for diagnostic purposes. The changes of critical speeds and natural modes might initiate an inspection of the tested machine.

6. References

[1] Kozánek J (1980) Parameter evaluation of a transfer function out of measured data, PhD thesis (In Czech). Prague, Institute of Thermomechanics, Academy of Sciences of the Czech Republic.

[2] Heylen W, Lammens S, Sas P (1994) Modal Analysis Theory and Testing. Leuven, Katholieke Universiteit Leuven.

[3] Balda M (2000) Identification of large-scale structures. In Křen J (Ed) *Computational Mechanics 2000, Proceedings of the 16th Conference with International Participation*, Nečtiny. pp 29-36. Pilsen: University of West Bohemia, ISBN 80-7082-652-5.

Appendix A: Frequency response matrix

It is possible to rewrite the system of second order equations (1) into first order ones. The Equation (1) complemented by the identity $\boldsymbol{M}\,\dot{\boldsymbol{q}}(t) = \boldsymbol{M}\,\dot{\boldsymbol{q}}(t)$ gives

$$\underbrace{\begin{bmatrix} \boldsymbol{M}\,, & \boldsymbol{O} \\ \boldsymbol{O}\,, & \boldsymbol{M} \end{bmatrix}}_{\boldsymbol{M}_s} \underbrace{\begin{bmatrix} \dot{\boldsymbol{q}}(t) \\ \ddot{\boldsymbol{q}}(t) \end{bmatrix}}_{\dot{\boldsymbol{v}}_s(t)} + \underbrace{\begin{bmatrix} \boldsymbol{O}\,, & -\boldsymbol{M} \\ \boldsymbol{K}\,, & \boldsymbol{B} \end{bmatrix}}_{-\boldsymbol{A}_s} \underbrace{\begin{bmatrix} \boldsymbol{q}(t) \\ \dot{\boldsymbol{q}}(t) \end{bmatrix}}_{\boldsymbol{v}_s(t)} = \underbrace{\begin{bmatrix} \boldsymbol{o} \\ \boldsymbol{f}(t) \end{bmatrix}}_{\boldsymbol{u}(t)}\,. \tag{21}$$

Deflections of the rotors may to be expressed as a function of the vector $\boldsymbol{v}$ in the form of the following linear combination

$$\boldsymbol{q}(t) = \boldsymbol{C}_s\, \boldsymbol{v}_s(t) + \boldsymbol{D}_s\, \boldsymbol{f}(t)\,. \tag{22}$$

Both Equations (21) and (22) rewritten together create a system known in the control theory as state space equations, which are in a slightly modified version of the form

$$\begin{bmatrix} \boldsymbol{M_s} & , \boldsymbol{O_{2n,n}} \\ \boldsymbol{O_{n,2n}} , & \boldsymbol{I_n} \end{bmatrix} \begin{bmatrix} \dot{\boldsymbol{v}}_s(t) \\ \boldsymbol{q}(t) \end{bmatrix} = \begin{bmatrix} \boldsymbol{A_s} \, , \boldsymbol{B_s} \\ \boldsymbol{C_s} \, , \boldsymbol{D_s} \end{bmatrix} \begin{bmatrix} \boldsymbol{v}_s(t) \\ \boldsymbol{f}(t) \end{bmatrix}, \tag{23}$$

with matrices

$$\begin{aligned} \boldsymbol{M}_s &= \begin{bmatrix} \boldsymbol{M} \, , \boldsymbol{O_n} \\ \boldsymbol{O_n} \, , \, \boldsymbol{M} \end{bmatrix}, \qquad \boldsymbol{A}_s = \begin{bmatrix} \boldsymbol{O_n} \, , \; \boldsymbol{M} \\ -\boldsymbol{K} \, , -\boldsymbol{B} \end{bmatrix}, \qquad \boldsymbol{B}_s = \begin{bmatrix} \boldsymbol{O}_n \\ \boldsymbol{I}_n \end{bmatrix}, \\ \boldsymbol{v}_s &= \begin{bmatrix} \boldsymbol{q}(t) \\ \dot{\boldsymbol{q}}(t) \end{bmatrix}, \qquad \boldsymbol{C}_s = [\, \boldsymbol{I}_n \, , \, \boldsymbol{O}_n \,] \, , \qquad \boldsymbol{D}_s = \boldsymbol{O}_n \, . \end{aligned} \tag{24}$$

The characteristic equation corresponding to (21) leads to the eigenvalue problem, the solution of which yields one diagonal spectral matrix $\boldsymbol{S}$ composed of eigenvalues s_ν and two modal matrices, $\boldsymbol{V}$ and $\boldsymbol{W}$, corresponding to it, containing right-hand-side eigenvectors $\boldsymbol{v}_\nu$ and left-hand-side eigenvectors $\boldsymbol{w}_\nu$, respectively. The Fourier transform applied to Equation (23) with zero initial conditions gives

$$\boldsymbol{q}(p) = \underbrace{\{\boldsymbol{C}_s \, [\, p \, \boldsymbol{M}_s - \boldsymbol{A}_s \,]^{-1} \, \boldsymbol{B}_s + \boldsymbol{D}_s\}}_{\boldsymbol{G}(p)} \, \boldsymbol{f}(p) \, . \tag{25}$$

The frequency response matrix may be expressed after using the formulae for matrices $\boldsymbol{B}_s$, $\boldsymbol{C}_s$, $\boldsymbol{D}_s$ and both conditions of ortho-normality $\boldsymbol{W}^H \boldsymbol{M}_s \boldsymbol{V} = \boldsymbol{I}_{2n}$ and $\boldsymbol{W}^H \boldsymbol{A}_s \boldsymbol{V} = \boldsymbol{S}$ as

$$\boldsymbol{G}(p) = \underbrace{[\, \boldsymbol{I}_n \, , \, \boldsymbol{O}_n \,] \, \boldsymbol{V}}_{\boldsymbol{V}_q} \, [\, p \, \underbrace{\boldsymbol{W}^H \boldsymbol{M}_s \, \boldsymbol{V}}_{\boldsymbol{I}_{2n}} - \underbrace{\boldsymbol{W}^H \boldsymbol{A}_s \, \boldsymbol{V}}_{\boldsymbol{S}} \,]^{-1} \; \underbrace{\boldsymbol{W}^H \begin{bmatrix} \boldsymbol{I}_n \\ \boldsymbol{O}_n \end{bmatrix}}_{\boldsymbol{W}_q^H} \, . \tag{26}$$

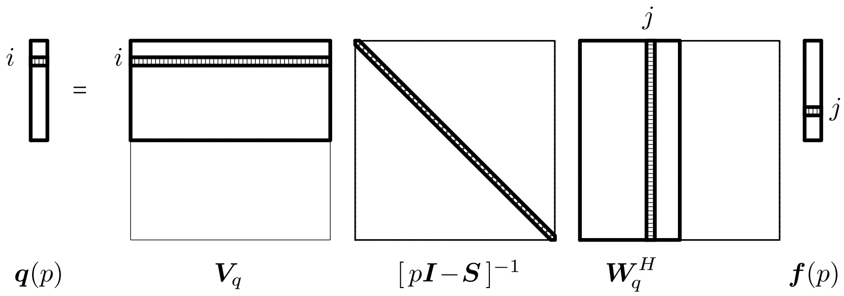

Figure 7: A scheme of generating an element of the response vector

Hence, the frequency response matrix may be written not only as the function of the coefficient matrices $\boldsymbol{M}$, $\boldsymbol{B}$, $\boldsymbol{K}$, but also in terms of spectral and modal matrices $\boldsymbol{S}$, $\boldsymbol{V}$, $\boldsymbol{W}$:

$$\boldsymbol{G}(p) = \boldsymbol{V}_q \, [\, p \, \boldsymbol{I}_{2n} - \boldsymbol{S} \,]^{-1} \, \boldsymbol{W}_q^H \tag{27}$$

Matrices $\boldsymbol{V}_q$ and $\boldsymbol{W}_q$ contain only the deflection submatrices.

Appendix B: Global identification of matrices $\boldsymbol{S}$, $\boldsymbol{V}$ and $\boldsymbol{W}$

Should n consecutive arbitrary independent excitations be applied virtually in n selected points of the system, and the excitation vectors build a matrix time series $\boldsymbol{F}(\kappa T) \in \mathcal{R}^{n,n}$, the corresponding matrix time series of responses

$$\boldsymbol{Q}(kT) \;=\; T \sum_{\kappa=0}^{k} \boldsymbol{G}((k-\kappa)T) \, \boldsymbol{F}(\kappa T) \;=\; T\boldsymbol{V} \sum_{\kappa=0}^{k} \exp((k-\kappa) \, \boldsymbol{S}T) \, \boldsymbol{W}^H \, \boldsymbol{F}(\kappa T) \tag{28}$$

Let Dirac impulses be applied for an excitation. This means that the excitation matrix time series becomes $\boldsymbol{F}(0) = \boldsymbol{I}_n$ and $\boldsymbol{F}(\kappa T) = \boldsymbol{O}_n$ for $\kappa > 0$. This excitation would generate matrix time series of impulse responses. Now, let us try to find additional excitation $\boldsymbol{F}(\kappa T) \neq \boldsymbol{O}_n$ for $1 \leq \kappa \leq \mu$ that would stop the vibration of the system caused by $\boldsymbol{F}(0) = \boldsymbol{I}_n$. It means that we require the response $\boldsymbol{Q}(\kappa T) = \boldsymbol{O}_{m,n}$ for $\kappa > \mu$. Should the mechanical system be linear as described by the equation (1) and controllable from a selected set of points, the number of periods for stopping vibrations is $\mu = 2$ provided that the excitation has been applied at every point. Should the number of excitation points n be smaller than number of degrees of freedom m, the number of periods for stopping the system is

$$\mu \geq \frac{2 \, n_f}{n} = \frac{n_e}{n} \, , \tag{29}$$

where n_f is the number of natural frequencies in the interval of observation, and n_e the corresponding number of eigenvalues. The condition $\boldsymbol{Q}(\kappa T) = \boldsymbol{O}_{m,n}$ for $\kappa > 0$ leads to the over-determined system of equations

$$\begin{bmatrix} \boldsymbol{G}_{\mu+1}\,, & \boldsymbol{G}_{\mu}\,, & \cdots\,, & \boldsymbol{G}_1 \\ \boldsymbol{G}_{\mu+2}\,, & \boldsymbol{G}_{\mu+1}\,, & \cdots\,, & \boldsymbol{G}_2 \\ \vdots\,, & \vdots\,, & , & \vdots \\ \boldsymbol{G}_{N-1}\,, & \boldsymbol{G}_{N-2}\,, & \cdots\,, & \boldsymbol{G}_{N-\mu-1} \end{bmatrix} \begin{bmatrix} \boldsymbol{I}_n \\ \boldsymbol{F}_1 \\ \vdots \\ \boldsymbol{F}_\mu \end{bmatrix} = \begin{bmatrix} \boldsymbol{O}_{m,n} \\ \boldsymbol{O}_{m,n} \\ \vdots \\ \boldsymbol{O}_{m,n} \end{bmatrix}, \tag{30}$$

solution of which is

$$\begin{bmatrix} \boldsymbol{F}_1 \\ \boldsymbol{F}_2 \\ \vdots \\ \boldsymbol{F}_\mu \end{bmatrix} = - \begin{bmatrix} \boldsymbol{G}_{\mu}\,, & \boldsymbol{G}_{\mu-1}\,, & \cdots\,, & \boldsymbol{G}_1 \\ \boldsymbol{G}_{\mu+1}\,, & \boldsymbol{G}_{\mu}\,, & \cdots\,, & \boldsymbol{G}_2 \\ \vdots\,, & \vdots\,, & , & \vdots \\ \boldsymbol{G}_{N-2}\,, & \boldsymbol{G}_{N-3}\,, & \cdots\,, & \boldsymbol{G}_{N-\mu-1} \end{bmatrix}^{+} \begin{bmatrix} \boldsymbol{G}_{\mu+1} \\ \boldsymbol{G}_{\mu+2} \\ \vdots \\ \boldsymbol{G}_{N-1} \end{bmatrix}. \tag{31}$$

The second right-hand side of the equation (18) multiplied by $\boldsymbol{V}^{+}/T$ yields the following homogenous system of algebraic equations

$$\begin{bmatrix} \boldsymbol{I}_n\,, \boldsymbol{F}_1^H\,, \boldsymbol{F}_2^H\,, \cdots, \boldsymbol{F}_\mu^H \end{bmatrix} \begin{bmatrix} \boldsymbol{W}\exp^H[(\mu+1)\boldsymbol{S}T] \\ \boldsymbol{W}\exp^H(\mu\boldsymbol{S}T) \\ \vdots \\ \boldsymbol{W}\exp^H(\boldsymbol{S}T) \end{bmatrix} = \boldsymbol{O}_n\,. \tag{32}$$

It is convenient to introduce new symbols for submatrices

$$\boldsymbol{Z} = \exp^H(\boldsymbol{S}T) \qquad \text{and} \qquad \boldsymbol{E}_\kappa = \boldsymbol{W}\,\boldsymbol{Z}^\kappa\,. \tag{33}$$

Hence, the equation (32) may be rewritten into the following form:

$$\begin{bmatrix} -\boldsymbol{F}_1^H\,, & -\boldsymbol{F}_2^H\,, & \cdots\,, & -\boldsymbol{F}_{\mu-1}^H\,, & -\boldsymbol{F}_\mu^H \\ \boldsymbol{I}_n\,, & \boldsymbol{O}_n\,, & \cdots\,, & \cdots\,, & \boldsymbol{O}_n \\ \boldsymbol{O}_n\,, & \boldsymbol{I}_n\,, & \ddots\,, & \cdots\,, & \vdots \\ \vdots\,, & \ddots\,, & \ddots\,, & \ddots\,, & \vdots \\ \boldsymbol{O}_n\,, & \cdots\,, & \boldsymbol{O}_n\,, & \boldsymbol{I}_n\,, & \boldsymbol{O}_n \end{bmatrix} \begin{bmatrix} \boldsymbol{E}_\mu \\ \boldsymbol{E}_{\mu-1} \\ \vdots \\ \boldsymbol{E}_2 \\ \boldsymbol{E}_1 \end{bmatrix} = \begin{bmatrix} \boldsymbol{E}_\mu \\ \boldsymbol{E}_{\mu-1} \\ \vdots \\ \boldsymbol{E}_2 \\ \boldsymbol{E}_1 \end{bmatrix} \boldsymbol{Z}\,, \tag{34}$$

which is a generalized eigenvalue problem of the type $\boldsymbol{A}\,\boldsymbol{E} = \boldsymbol{E}\,\boldsymbol{Z}$, where $\boldsymbol{Z}$ is the spectral matrix of $\boldsymbol{A}$ and $\boldsymbol{E}$ a modal matrix. Since the sampling frequency $f_s = 1/T$, an estimate $\hat{\boldsymbol{S}}$ of the spectral matrix $\boldsymbol{S}$ of the original problem may be found from the definition of the matrix $\boldsymbol{Z}$ in (33) as

$$\hat{\boldsymbol{S}} = f_s\, ln\, \boldsymbol{Z}^H \tag{35}$$

The estimated spectral matrix $\hat{\boldsymbol{S}}$ may include additional eigenvalues that do not belong to the original system in cases that the number of eigenvalues required has been higher than in reality.

The simplest way how to obtain the modal matrix of left-hand-side vectors $\boldsymbol{W}$ is based on the second expression in (33) which gives

$$\boldsymbol{W} = \boldsymbol{E}_1\,\boldsymbol{Z}^{+} \tag{36}$$

The modal matrix $\boldsymbol{V}$ of right-hand-side vectors is calculated from the equation (16) which must hold for every k. Thus, we get an over-determined system, the solution of which is

$$\boldsymbol{V} = \left[\boldsymbol{G}(kT)\right]\left[\exp(k\boldsymbol{S}T)\,\boldsymbol{W}^H\right]^{+} \qquad \text{for} \qquad k = 0, 1, \ldots, N-1 \tag{37}$$

Acknowledgment: The results presented here were supported by the Grant Agency of the Czech Republic under contracts 101/00/0898 and 101/02/0043.